ELSEVIER

www.elsevier.nl/locate/jorganchem

Journal of Organometallic Chemistry 601 (2000) 114–125

Journal of Organometallic Chemistry

para-Substituted diphenylborylated organocobaloximes: effects of substituents on conformation and redox properties

Fioretta Asaro, Renata Dreos *[1], Giorgio Nardin, Giorgio Pellizer, Silvia Peressini, Lucio Randaccio *[2], Patrizia Siega, Giovanni Tauzher, Claudio Tavagnacco

Dipartimento di Scienze Chimiche, Università Degli Studi di Trieste, via Licio Giorgieri 1, I-34127 Trieste, Italy

Received 8 October 1999; received in revised form 24 November 1999; accepted 5 January 2000

Abstract

Some new derivatives of organocobaloximes containing *para*-substituted diphenylboryl groups, $RCo(DH)_{2-n}(DB(p\text{-}XPh)_2)_nL$ (R = alkyl or aryl group, L = *N*-MeIm, Py or H_2O, X = OCH_3, CH_3 or Cl, $n = 1$ or 2) have been synthesized. The X-ray structures and the ^{1}H-NMR spectra are compared with those of the corresponding $RCo(DH)_{2-n}(DBPh_2)_nL$ and $RCo(DBF_2)_2L$ complexes. The insertion of X groups in the phenyl rings does not significantly affect the equatorial Co–N distances, whereas the Co–Py distances increase slightly in the order $(DB(p\text{-}OCH_3Ph)_2)_2 < (DB(p\text{-}ClPh)_2)_2 < (DBF_2)_2$. ^{1}H-NMR spectra suggest that the conformational distribution in solution is similar to that observed in the corresponding BPh_2 derivatives. Electrochemical studies on the corresponding $MeCo(DB(p\text{-}XPh)_2)_2H_2O$ compounds show a mono-electron Co(III)/Co(II) transfer reaction followed by two parallel reactions: (a) mono-electron Co(II)/Co(I) transfer; (b) homolytic dissociation of the Co–C bond with the formation of Co(I) species, the relative rates of the two processes being dependent on X. As the electron-withdrawing power of the equatorial ligand increases, the reduction potentials associated with both Co(III)/Co(II) and Co(II)/Co(I) processes shift towards more positive values, indicating a decrease of electron density on the Co atom. The effects are comparable with those observed by changing the axial ligands.

Keywords: Organocobaloximes; *p*-Substituted diphenylborinic groups; Conformational equilibria; X-ray structures; Electrochemical properties

1. Introduction

Bis(dimethylglyoximate) complexes in which the protons of the oxime groups are formally replaced by boryl bridges are well known [1]. In organocobaloximes, $RCo(III)(DH)_2L$, the replacement of the O···H···O bridge with BF_2, $RCo(DBF_2)_2L$, affects both the geometry of the complexes [2] and the electron density at the central metal ion [3]. Organocobaloximes containing BPh_2 bridges, $RCo(DH)_{2-n}(DBPh_2)_nL$ (R = alkyl or aryl group, L = neutral ligand, $n = 1$ or 2), may adopt different conformations in solution and ^{1}H-NMR spectroscopy allows the conformational equilibrium to be studied by exploiting the anisotropy effects both of the BPh_2 phenyls and of the axial ligands [4,5]. The conformational equilibrium shifts from 'up' to 'down' for the monoborylated derivatives (Scheme 1), and from 'up–down' to 'down–down' for the diborylated ones with increasing steric bulk of R (Scheme 2) [4]. Pure 'up–up' forms have not been evidenced yet either in solution or in solid state, if the pentacoordinate Co(I) species, $PyCo(DBF_2)_2^-$, is excluded [6].

X-ray diffraction studies show that when the complex assumes a conformation in which at least one phenyl of the BPh_2 group faces a planar neutral ligand L, the latter is forced into an orientation that bisects the five-membered rings of the equatorial moiety. This orientation is quite unusual in cobaloximes, but is generally observed in iminocobaloximes, $\{RCo[(DO)(DOH)pn]L\}^+$ cations, and leads to a lengthening of the axial Co–N [7,8]. Ligands with good π-acceptor properties stabilize 'down–down' conformation [9], so confirming the role of π–π interactions between the phenyls of the BPh_2 bridge and the axial ligands, as previously found for $LFe(II)(DBPh_2)_2L'$ systems [5].

[1]*Corresponding author. Tel.: +39-40-6763902; fax: +39-40-6763903; e-mail: dreos@univ.trieste.it

[2]*Corresponding author. Tel.: +39-40-6763902; fax: +39-40-6763903.

0022-328X/00/$ - see front matter
PII: S0022-328X(00)00043-7

In order to investigate the effects of a *para* substitution in the phenyls on conformation and electron affinity of the redox center, we report here the synthesis and the characterization of several derivatives of organocobaloximes containing *para*-substituted diphenylboryl groups.

2. Experimental

$RCo(DH)_2L$ [10], $RCo(DBF_2)_2H_2O$ [10] and $RCo(DBPh_2)_2L$ [4] were synthesized as previously described.

The $(p\text{-ClPh})_2BOH$, $(p\text{-OCH}_3\text{Ph})_2BOH$ and $(p\text{-CH}_3\text{Ph})_2BOH$ acids were prepared according to the procedure of Povlock and Lippincott [11]. Solvent and other reagents have been commercially purchased.

2.1. Syntheses

We report the general procedure for the synthesis of the complexes $RCo(DH)_{2-n}(DB(p\text{-XPh})_2)_nL$ (R = alkyl or aryl group, L = *N*-MeIm, Py, or H_2O, X = OCH_3, CH_3 or Cl, $n = 1$ or 2). The reaction time depends on both the bulk of the axial ligands [4] and the nature of the substituent X in *para* position in the phenyls, being considerably longer for the *p*-Cl derivatives. The completeness of the reaction was checked by ^{1}H-NMR spectroscopy. The complexes were identified by ^{1}H- and ^{13}C-NMR spectroscopy and, in some cases, by elemental analysis.

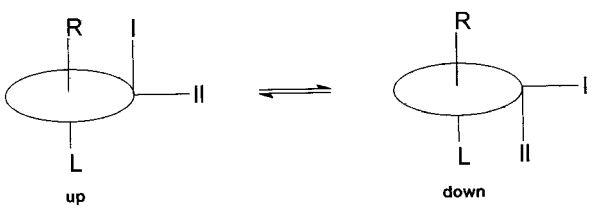

Scheme 1.

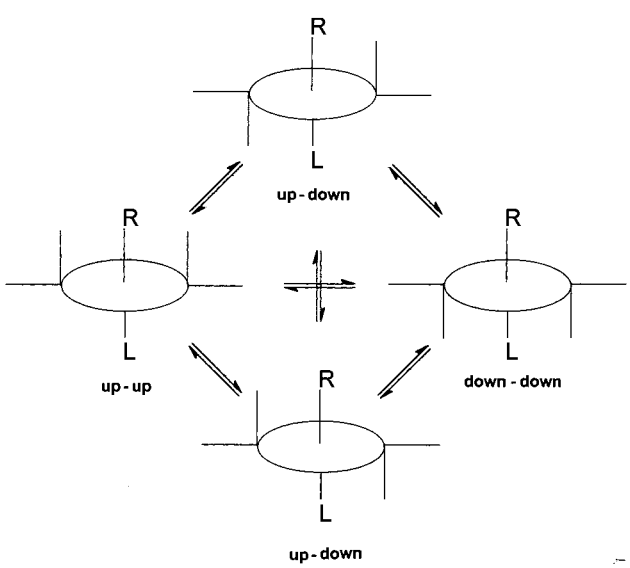

Scheme 2.

2.1.1. $RCo(DH)(DB(p\text{-XPh})_2)L$ derivatives (L = *N*-MeIm or Py)

A total of 0.1 g $RCo(DH)_2L$ was dissolved in about 50 ml of CH_2Cl_2 and an equimolar amount of borinic acid was added, together with a small excess of L in order to avoid the dissociation of the axial base. The solution was heated at 35°C for times varying from 1 to 3 days. Partial evaporation of the solvent and the addition of 2–3 ml of *i*-PrOH afforded yellow powders, which were recrystallized from CH_2Cl_2/*i*-PrOH.

2.1.2. $RCo(DB(p\text{-XPh})_2)_2L$ derivatives (L = *N*-MeIm or Py)

A total of 0.1 g of the corresponding $RCo(DH)_2L$ was dissolved in about 50 ml of CH_2Cl_2 with an eight-fold excess of the borinic acid. Some drops of L were added in order to avoid the dissociation of the axial base. The solution was heated at 35°C for times varying from 1 to 3 days. Partial evaporation of the solvent and the addition of 2–3 ml of *i*-PrOH afforded yellow powders, which were recrystallized from CH_2Cl_2/*i*-PrOH.

2.1.3. $RCo(DB(p\text{-XPh})_2)_2H_2O$ derivatives

A total of 0.1 g of the corresponding $RCo(DH)_2H_2O$ was suspended in about 50 ml of CH_2Cl_2 saturated with water; then acetone was added until dissolution. Borinic acid in molar ratio 3:1 with complex was added to the solution, which was heated at 40°C for 1 or 2 days. Partial evaporation of the solvent afforded the products. All the complexes were recrystallized from CH_2Cl_2/*i*-PrOH.

2.1.4. $MeCo(DB(p\text{-}OCH_3Ph)_2)_2H_2O$

A total of 0.1 g $MeCo(DBp\text{-}OCH_3Ph_2)_2N$-MeIm was dissolved in 40 ml of dimethylsulfoxide. The solution was acidified with $HClO_4$ (pH about 3) and left for about 10 min. Addition of water caused the precipitation of $MeCo(DB(p\text{-}OCH_3Ph)_2)_2H_2O$, sparingly soluble in water.

2.2. NMR measurements

^{1}H- and ^{13}C-NMR spectra were recorded on a JEOL EX-400 (^{1}H at 400 MHz and ^{13}C at 100.4 MHz) from $CDCl_3$ solutions with TMS as internal standard.

2.3. X-ray structure determinations

Crystallographic data for $MeCo(DH)(DBPh_2)Py$ (**1**), $MeCo(DBPh_2)_2Py$ (**2**), $MeCo(DB(p\text{-ClPh})_2)_2Py$ (**3**), and

Table 1
Crystal data and experimental conditions of complexes **1**, **2**, **3**, and **4**

	1	**2**	**3**	**4**
Empirical formula	$C_{26}H_{31}BCoN_5O_4$	$C_{38}H_{40}B_2CoN_5O_4$	$C_{38}H_{36}B_2Cl_4CoN_5O_4$	$C_{42}H_{48}B_2CoN_5O_8 \cdot CH_2Cl_2$
Formula weight	547.3	711.3	849.1	916.3
Crystal dimensions (mm)	$0.2 \times 0.5 \times 0.2$	$0.2 \times 0.2 \times 0.7$	$0.2 \times 0.3 \times 0.2$	$0.2 \times 0.4 \times 0.7$
Unit cell dimensions				
a (Å)	8.651(2)	8.353(2)	16.740(3)	9.305(2)
b (Å)	16.275(7)	10.479(3)	10.262(2)	15.930(4)
c (Å)	18.727(4)	11.627(3)	23.459(3)	16.607(4)
α (°)	90	66.82(3)	90	70.38(2)
β (°)	93.57	73.27(2)	99.41(10)	73.44(2)
γ (°)	90	72.12(2)	90	83.57(2)
V (Å^3)	2633(1)	874.0(4)	3976(1)	2222.1(9)
Z	4	1	4	2
Space group	$P2_1/n$	$P\bar{1}$	$P2_1/n$	$P\bar{1}$
Absorption correction	ψ-scan	ψ-scan	ψ-scan	ψ-scan
Independent reflections	3831	3816	2489	4215
Parameters refined	159	252	247	559
R_1	0.093	0.071	0.106	0.087
wR_2	0.183	0.172	0.184	0.213
Goodness-of-fit	0.94	1.15	0.92	1.12

Table 2
Comparative geometrical values for $MeCo(DH)_{2-n}(DB(p\text{-}XPh)_2)_n$ Py

X	n	Complex	Co–N_{eq}(mean)	Co–C	Co–N_{ax}	O···O	d(Co)
H(N-MeIm)	1	Ref. [4b]	1.869(8) [a] 1.878(8) [b]	1.995(12)	2.014(9)	2.469 [a] 2.510 [b]	0.009
H	1	**1**	1.876(9) [a] 1.869(10) [b]	2.000(11)	2.083(9)	2.438 [a] 2.534 [b]	0.033
H	2	**2**	1.867(4)	2.098(5) [c]	2.098(5) [c]	2.526	0
Cl	2	**3**	1.864(8)	1.998(9)	2.106(8)	2.542 2.528	0.076
OCH_3	2	**4**	1.867(5)	2.032(6)	2.086(6)	2.524 2.519	0.082

[a] On the side of BPh_2 group.
[b] On the side of the oxime bridge.
[c] The values are a consequence of the disorder due to the location of Co on the symmetry center, so that they cannot be discussed.

$MeCo(DB(p\text{-}OCH_3Ph)_2)_2Py$ (**4**) are collected in Table 1. Structural data of interest are given in Table 2.

Crystals of complexes **1**–**4**, suitable for X-ray structure analysis, were obtained by slow diffusion of CH_2Cl_2 solutions in *i*-PrOH; however, in the case of complex **1** the size of the crystals was very small. Preliminary examination and data collection were performed with Mo–K_α radiation ($\lambda = 0.70930$ Å) on an Enraf–Nonius CAD4 diffractometer with a graphite monochromator. Empirical absorption correction, based on ψ-scan data, was applied. The structures were solved by conventional Patterson, Fourier analysis and refined by the least-square methods. H atoms were located at calculated positions. Final positional parameters and B values are reported as supplementary material. All calculations were performed using SHELXS and SHELXL programs [12].

2.4. Electrochemical measurements

All the electrochemical measurements were made in dimethylsulfoxide (DMSO) solution that was prepared by holding the commercial product over NaOH for 3 h at 90°C and distilling it at reduced pressure [13]. Tetraethylammonium perchlorate (TEAP) vacuum dried at 30°C was the supporting electrolyte. (**CAUTION**: perchlorate salts are potentially explosive and should be handled with great care.)

Polarographic and cyclic voltammetry (CV) measurements were performed using an Amel 552 Potentiostat/Galvanostat connected with an Amel 568 function generator. For fast CV a home-made potentiostat [14] equipped with positive feedback and driven by a Hewlett–Packard function generator 3314A was used. The measurements were always made at 25 ± 0.1°C under Ar or N_2 atmosphere in a three-electrode thermostated

jacket cell. A dropping mercury electrode (DME) was used as the working electrode for polarography, while a Metrohom 663 VA Stand for Hg was used for CV. The reference was a saturated aqueous NaCl | calomel electrode (SCE), contained in a glass tube separated from the solution by a glass frit of medium porosity which was located very close to the tip of the working electrode to minimize the ohmic drop, and filled with the supporting electrolyte solution. The counter electrode was a Pt ring or rod directly dipped in the solution. The peak potentials and currents were evaluated after subtraction of the background current.

Controlled potential reduction (CPR) was made on a stirred Hg pool of about 12 cm^2 surface area: in that case the counter electrode was separated from the solution by a glass frit filled with the supporting electrolyte solution. The charge passed was determined by an Amel 731 integrator.

3. Results

3.1. Syntheses

The reactivity of organocobaloximes with *para*-substituted diphenylborinic acids strictly resembles that with diphenyl borinic anhydride [4]. When L is a nitrogen base, generally, either mono or diphenylborilated derivatives could be isolated, depending on the acid/complex ratio. In some cases, for bulky axial ligands such as phenyl or *trans*-β styryl, the diborylated complex could not be isolated and NMR spectra always revealed mixtures of mono and diborylated complexes. When L was H_2O only diphenylborylated complexes were recovered. The aquaderivatives were generally obtained by heating the corresponding organoaquacobaloxime in presence of borinic acid, but for MeCo(DB(p-$OCH_3Ph)_2)_2H_2O$ this method was unsuccessful, the reaction product being a complex containing one boryl bridge and one molecule of (p-$OCH_3Ph)_2BOH$ coordinated *trans* to methyl. Similar complexes have been evidenced previously, when organocobaloximes were treated with diphenylborinic anhydride in anhydrous solvent [15]. Authentic MeCo(DB(p-$OCH_3Ph)_2)_2H_2O$ could be recovered by hydrolysis of MeCo(DB(p-$OCH_3Ph)_2)_2N$-MeIm in DMSO and successive addition of water to the reaction mixture.

3.2. Structural results

The ORTEP drawings of the complexes **1** and **2** are depicted in Fig. 1 and those of **3** and **4** in Fig. 2. In complex **1**, the axial CH_3 group faces the axial phenyl of the BPh_2 unit and the pyridine nearly bisects the six-membered ring (orientation A), as previously found in the analogous MeCo(DH)($DBPh_2$)N-MeIm complex [4]. In complex **2** the cobalt atom lies on a crystallographic symmetry center so that the equatorial moiety shows an 'up–down' conformation and the axial ligands are superimposed. The pyridine ligand is rotated by about 25° with respect to the ideal face-to-face contact with the axial phenyl of the BPh_2 unit (orientation B).

The torsion angles $\delta = N2'–Co–N5–C17$ and $\delta' = N1–Co–N5–C17$ of -17 and 65°, respectively, indicate the relative position of the pyridine plane with respect to the equatorial moiety.

Complexes **3** and **4** show a very similar 'up–down' extended chair conformation. The equatorial moieties of **3** and **4** have an ca. C_{2h} symmetry, if the orientation of the equatorial p-OCH_3Ph rings at boron is not considered (Fig. 2). The pyridine, in orientation B, faces the axial p-ClPh ring in **3** and the analogous p-OCH_3Ph ring in complex **4**. The corresponding δ and δ' values are -33.8 and 47.8 for **3** and 34.8 and -47.2° for **4**, respectively. Consequently, the plane of the pyridine ring in **3** and **4** is nearly perpendicular to the plane defined by the cobalt and two boron atoms.

Comparison of the O···O distances in **1** indicates a shortening of about 0.1 Å on the side of the oxime bridge (Table 2). In **2**, **3** and **4** all the O···O distances are very similar, being in the range 2.519–2.542 Å. The presence of one or two boron bridges or the insertion of substituents in the phenyl rings does not seem to affect significantly the equatorial Co–N bond distances (Table 2). Also the Co–CH_3 bond distances do not appear to be influenced by the nature of the equatorial ligand, the value of 2.098(5) for **2** being an artefact due to the axial CH_3/Py disorder imposed by the symmetry center. Only in **4** does the Co–C of 2.032(6) appear slightly but significantly longer than the values found in **1** and **3** (Table 2). The neutral ligand in **1** and in the analogous N-MeIm derivative [4] has orientation close to A, the Co–Py distances being 0.07 Å longer, due to the larger bulk of Py. This also affects the Co displacement out of the equatorial 4-N donors towards L, which is 0.033 Å in complex **1** and 0.009 Å in the N-MeIm analogue. It has been observed in cobaloximes and iminocobaloximes [7] that the Co–N_{axial} distances are appreciably affected by the orientation of the planar L ligand, being shorter in orientation A, as occurs in N-MeIm derivatives with $n = 1$ (2.014(9) Å), than in orientation B, as occurs in N-MeIm derivatives with $n = 2$ [4], (2.068(7) Å). Comparison of the analogous Py derivatives with $n = 1$ and 2, respectively (Table 2) is hampered by the disorder in **2**. The Co displacement out of the 4-N equatorial plane towards N pyridine atom varies from 0.03 Å in complex **1** to 0.08 Å in **3** and **4**. Only in **2**, owing to the special position of the metal, the cobalt atom lies in the coordination basal plane.

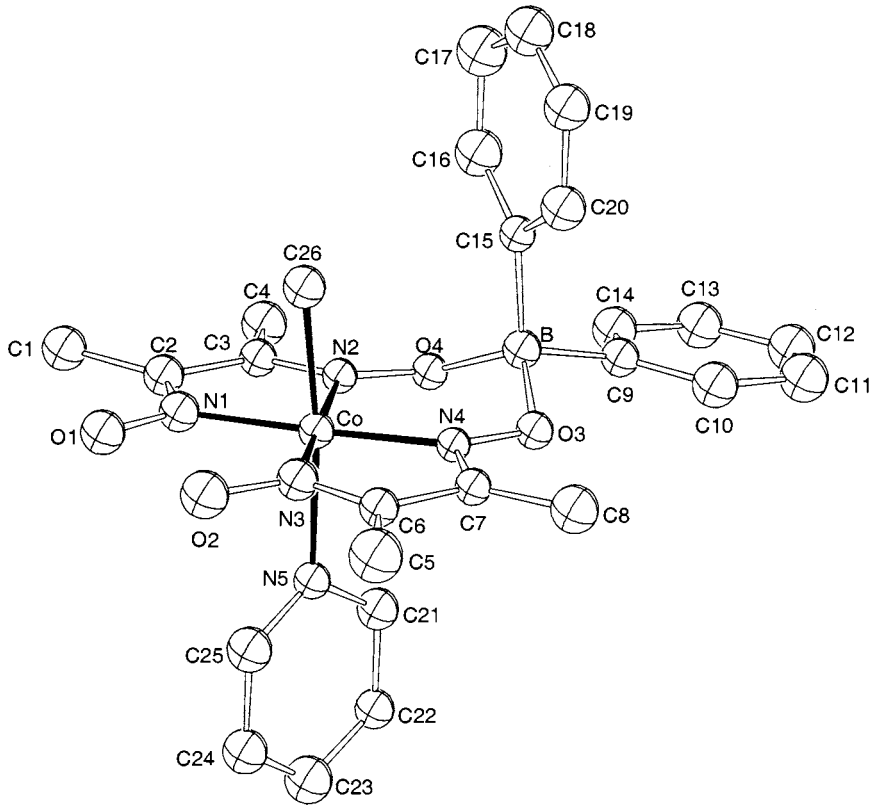

1

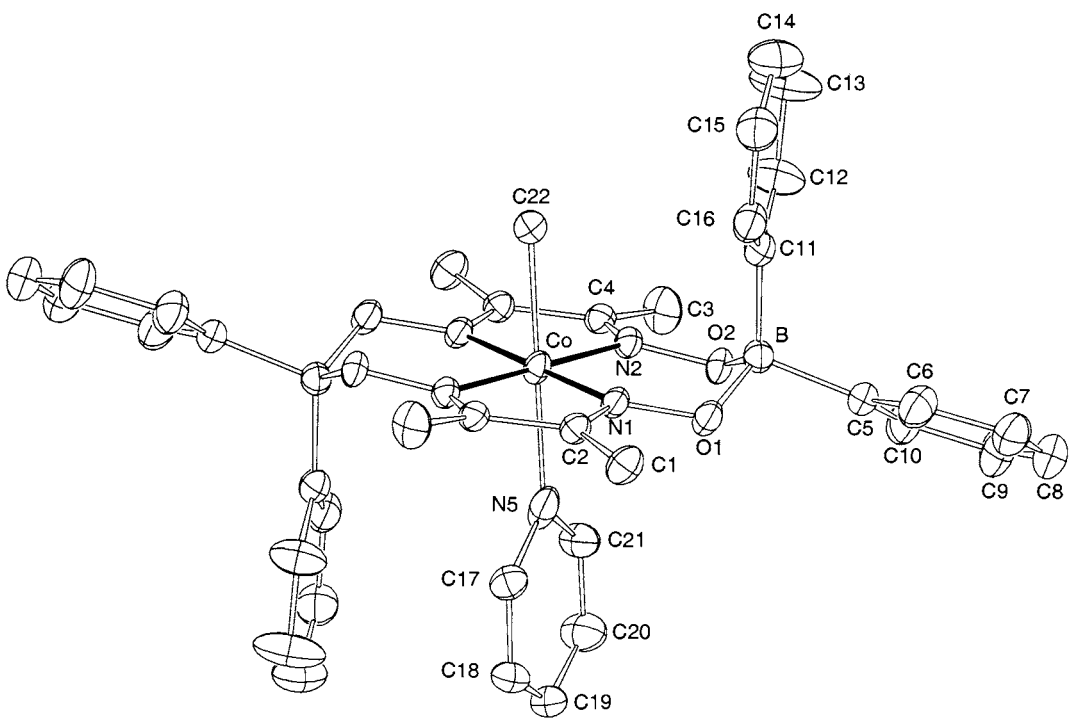

2

Fig. 1. The ORTEP drawing and the atom numbering scheme of the complexes $MeCo(DH)(DBPh_2)Py$ (**1**) and $MeCo(DBPh_2)_2Py$ (**2**) (thermal ellipsoids at 30% probability).

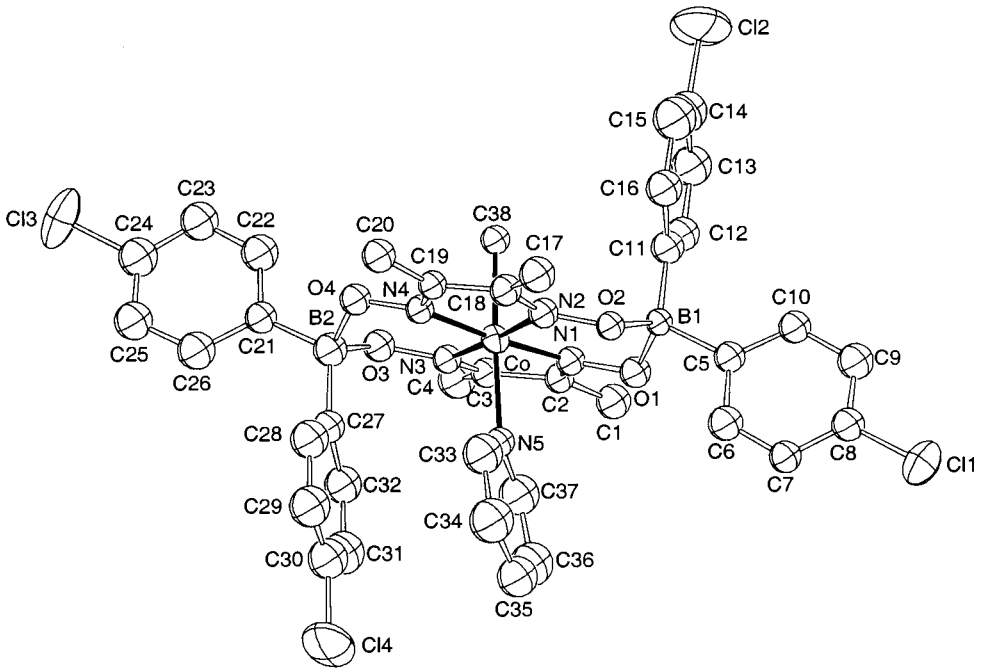

3

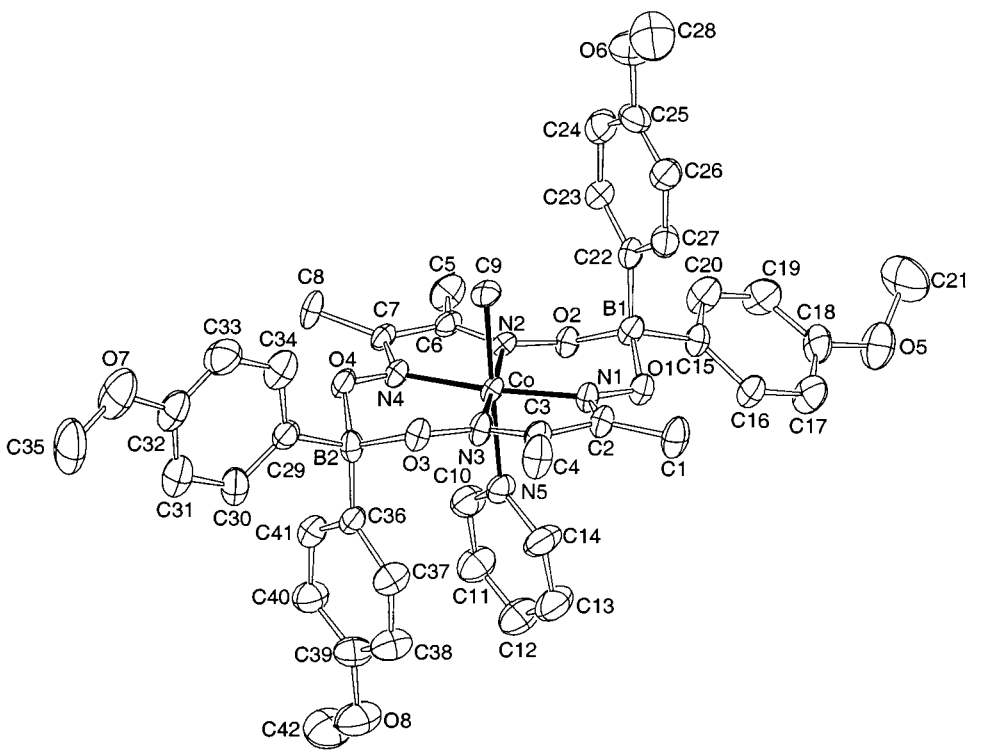

4

Fig. 2. The ORTEP drawing and the atom numbering scheme of the complexes $MeCo(DB(p\text{-}ClPh)_2)_2Py$ (**3**) and $MeCo(DB(p\text{-}OCH_3Ph)_2)_2Py$ (**4**) (thermal ellipsoids at 30% probability).

Table 3
^{1}H-NMR chemical shift of RCo(DH)$_n$(DB(*p*-XBPh)$_2$)$_{2-n}$*N*-MeIm complexes [a,b]

Complexes	R				CH_3 eq.	N-MeIm			B(*p*-XPh)$_2$		
	α	β	γ	δ		H-2	H-5, H-4	CH_3	*ortho*	*meta*	OCH_3
MeCo(DH)$_2$*N*-MeIm [c]	0.72				2.13	7.44	6.78, 6.94	3.66	7.18	6.74	
MeCo(DH)(DB(*p*-OCH_3Ph)$_2$)*N*-MeIm	0.22				2.15–2.36	7.40	6.72, 7.01	3.59	7.47	6.79	3.74–3.76
									7.09	7.20	
MeCo(DB(*p*-OCH_3Ph)$_2$)$_2$*N*-MeIm	0.42				2.41	6.02	6.46, 6.48	3.30	6.63	6.74	3.72–3.74
n-PrCo(DH)$_2$*N*-MeIm [c]	1.52	0.94	0.78		2.13	7.42	6.76, 6.95	3.62	7.29	6.69	
n-PrCo(DH)(DB(*p*-OCH_3Ph)$_2$*N*-MeIm	1.26	0.61	0.44		2.19–2.38	6.90	6.60, 6.73	3.48	7.29	6.76	3.74–3.75
									6.98	6.55	
n-PrCo(D(B*p*-OCH_3Ph)$_2$)$_2$*N*-MeIm	1.51	0.44	0.29		2.43	5.94	6.21, 6.24	3.24	7.24	6.75	3.69–3.73
n-BuCo(DH)$_2$*N*-MeIm [c]	1.52	0.87	1.18	0.78	2.12	7.42	6.75, 6.94	3.62	7.28	6.69	
n-BuCo(DH)(DB(*p*-OCH_3Ph)$_2$)*N*-MeIm	1.28	0.53	0.81	0.64	2.18–2.38	6.93	6.61, 6.75	3.48	7.29	6.75	3.74
									6.98	6.55	
n-BuCo(DB(*p*-OCH_3Ph)$_2$)$_2$*N*-MeIm	1.52			0.64	2.42	5.97	6.23, 6.25	3.25	7.24	6.74	3.70–3.73
PhCo(DH)$_2$*N*-MeIm [c]	7.39	6.89–6.94 (*m*+*p*)			2.04	7.57	6.79, 7.08	3.66	6.89	6.46	
PhCo(DH)(DB(*p*-OCH_3Ph)$_2$)$_2$*N*-MeIm	7.54				2.18–2.34	5.88	6.03, 6.35	3.29	7.54	6.86	3.69–3.79
									6.73	6.34	
PhCo(D(B*p*-OCH_3Ph)$_2$)$_2$*N*-MeIm	7.73 (*o*)	6.97 (*m*+*p*)			2.40	5.50	5.47, 5.33	3.01	7.41	6.80	3.66–3.77
MeCo(DH)(DB(*p*-ClPh)$_2$)*N*-MeIm	0.22				2.16–2.38	6.72		3.59	6.99	6.94	
MeCo(DB(*p*-ClPh)$_2$)$_2$*N*-MeIm	0.53				2.47	5.91	6.08, 6.37	3.36	7.20	7.14	
PhCo(DH)(DB(*p*-ClPh)$_2$)*N*-MeIm	7.45 (*o*)	6.92 (*m*+*p*)			2.20–2.36	6.40	5.93, 5.97	3.39	6.89	6.83	
PhCo(D(B*p*-ClPh)$_2$)$_2$*N*-MeIm	7.55 (*o*)	6.94 (*m*+*p*)			2.43	5.53	5.31, 5.66	3.15	7.53	7.24	
									6.75	6.75	
MeCo(DB(*p*-CH_3Ph)$_2$)$_2$*N*-MeIm	0.39				2.40	6.15	6.41, 6.51	3.27	7.41	7.20	2.24–2.20
									7.11	6.87	
PhCo(DH)(DB(*p*-CH_3Ph)$_2$)$_2$*N*-MeIm	7.52 (*o*)				2.18–2.35	5.95	6.00, 6.30	2.95	7.17	6.97	2.19–2.30
									6.87	6.67	
PhCo(D(B*p*-CH_3Ph)$_2$)$_2$*N*-MeIm	7.73 (*o*)				2.41	5.52	5.35, 5.29	2.95	7.52	7.09	2.14–2.20
									6.71	6.56	
									7.40	7.05	

[a] δ in ppm from TMS, $CDCl_3$ solutions.
[b] Some of the monoborylated complexes were not isolated but directly prepared in the NMR tube.
[c] From Ref. [4].

3.3. ^1H-NMR studies

3.3.1. Axial ligands

Only one set of signals is observed for each axial ligand because the interconversion among conformers is fast on the NMR time-scale in $CDCl_3$ solution at room temperature. The proton chemical shift of the methyl of *N*-MeIm has proved to be a valid parameter for investigating the conformational equilibria, because it responds almost exclusively to the through-space effects of the BPh_2 aromatic rings [4]. In the MeCo(DH)(DB(p-XPh)$_2$)*N*-MeIm compounds (X = OCH_3 and Cl) its resonance frequency does not depend significantly on X (Table 3). This indicates that the prevailing conformation is 'up', as already found for the parent compound (X = H) [4]. In the PhCo(DH)(DB(p-XPh)$_2$)*N*-MeIm complexes the methyl of *N*-MeIm is much more shielded, indicating that the 'down' conformation is preferred, like when X = H. In this case the magnitude of the shielding shows a clear dependence on X, decreasing in the order H ~ CH_3 > OCH_3 > Cl.

In the RCo(DB(p-XPh)$_2$)$_2$*N*-MeIm compounds the methyl of *N*-MeIm is more shielded that in the corresponding monoborylated species and the main conformation is 'up–down' for R = Me and 'down–down' for R = Ph, as for the derivatives with unsubstituted BPh_2 bridges. The effect decreases on changing X in the above reported order.

In the *n*-Pr and *n*-Bu derivatives, the R protons bonded to the γ carbon are affected only by B(p-XPh)$_2$ through-space effects [4]. The RCo(DH)$_{2-n}$(DB(p-OCH_3Ph)$_2$)$_n$*N*-MeIm (R = *n*-Pr and *n*-Bu) compounds behave like the corresponding ones with unsubstituted BPh_2 groups, except for the slightly smaller shielding both on the methyl of *N*-MeIm and on the protons at the γ carbons.

3.3.2. Equatorial ligand

The equatorial methyls in the RCo(DH)$_{2-n}$(DB(p-XPh)$_2$)$_n$*N*-MeIm resonate close to those of the corresponding complexes with X = H. Further insight is gained through examination of the spectra of the boryl bridge protons. All the compounds studied in this paper show the signals of two different phenyls, even those containing two boryl bridge. The spectral pattern of each phenyl reflects its fast exchange between the axial and the equatorial situations, the weights of which depend on the conformational equilibrium [4,5]. The proton spectra of B(p-XPh)$_2$ groups correspond to AA′BB′ spin systems but the extreme case of an A_4 spin system occurs for the more shielded phenyl of PhCo(DB(p-ClPh)$_2$)$_2$*N*-MeIm.

The shielding of the phenyl protons, beside on X, depends on the through-space effects of the axial ligands, and therefore on the conformation. This was exploited in order to determine the influence of R on the preferred conformation in solution. We have taken the difference between the chemical shifts of the protons of each X-substituted compound and those of the corresponding protons in the parent compounds (X = H). The values so obtained for a given position (*ortho* or *meta* to boron), and a given X are independent of R and of the number of boryl bridges (Table 4) and close to the values of substituent induced shifts reported in literature [16]. This implies that the through-space effects caused by the axial ligands are the same both in the compounds with X = CH_3, OCH_3 and Cl and in that with X = H, and confirms that the conformational equilibrium is substantially independent of X. Accordingly, the dependence on X of the shielding of *N*-MeIm methyl and of the γ protons of the *n*-Pr and *n*-Bu axial ligands (see above) reflects changes of magnetic anisotropy and electric dipoles due to substitution of the BPh_2 phenyls, rather than modifications of the conformational equilibrium.

Table 4
X-substituent-induced shifts on the phenyl protons in RCo(DH)$_{2-n}$(DB(p-XPh)$_2$)$_n$*N*-MeIm compounds

X	Δδ (ppm) [a]	
	Meta	*Ortho*
CH_3	−0.20	−0.15
OCH_3	−0.42	−0.12
Cl	−0.04	−0.11

[a] Δδ is the difference between the chemical shifts of the protons of the X-substituted compound and those of the corresponding protons in the parent compounds (X = H).

3.4. Electrochemical studies

The electrochemical studies were performed on a series of aquaderivatives: MeCo(DBF_2)$_2$$H_2O$ (**5**), MeCo(DB(p-ClPh)$_2$)$_2$$H_2O$ (**6**), MeCo(DB(p-OCH_3Ph)$_2$)$_2$$H_2O$ (**7**), MeCo($DBPh_2$)$_2$$H_2O$ (**8**), MeCo(DB(p-CH_3Ph)$_2$)$_2$-H_2O (**9**) and MeCo(DH)$_2$$H_2O$ (**10**).

All the measurements were carried out in DMSO, as this was the only solvent in which all the above complexes were sufficiently soluble.

3.4.1. Polarography

The polarography in DMSO and 0.1 M TEAP in the range from + 0.3 to − 2.0 V shows two distinct monoelectronic reduction waves that are associated with the Co(III)/Co(II) (wave **I**) and Co(II)/Co(I) (wave **II**) processes, respectively. Some polarographic characteristic data are summarized in Table 5[3]. The height of the

[3] Serious problems were sometimes encountered upon electrochemical reduction due to adsorption signals that limit the possibility of getting high-precision results, especially with MeCo(DB(p-ClPh)$_2$)$_2$$H_2O$ and MeCo($DBPh_2$)$_2$$H_2O$.

Table 5
Summary of polarographic and cyclic voltammetry data for $MeCo(chel)H_2O$ in DMSO and 0.1 M TEAP at 25°C

Complexes	Polarographic data						Cyclic voltammetry data [c]			
	Co(III)/Co(II)			Co(II)/Co(I)						
	$E_{1/2}$ (V)	Log plot [a]	n [b]	$E_{1/2}$ (V)	Log plot [a]	$i_l(\mathbf{I})/i_l(\mathbf{II})$	$E_{pc}(\mathbf{I})$ (V)	$\Delta E_p(\mathbf{I})$ (V)	$E_{pc}(\mathbf{II})$ (V)	$\Delta E_p(\mathbf{I})$ (V)
$MeCo(DBF_2)_2H_2O$ (**5**)	−0.75	Irrev	1	−1.17		8.6	−1.02			
$MeCo(DB(p\text{-}ClPh)_2)_2H_2O$ (**6**)	−0.89	Irrev		−1.09	Rev	1.58	−0.943	0.112	−1.12	0.066
$MeCo(DB(p\text{-}OCH_3Ph)_2)_2H_2O$ (**7**)	−0.96	Irrev		−1.20	Quasirev	1.04	−1.045	0.138	−1.215	0.054
$MeCo(DBPh_2)_2H_2O$ (**8**)	−0.96	Quasirev	1	−1.17	Quasirev	0.97	−1.044	0.168	−1.215	0.069
$MeCo(DB(p\text{-}CH_3Ph)_2)_2H_2O$ (**9**)	−0.99	Irrev	1	−1.25	Rev	0.93	−0.76	0.077	−1.213	
$MeCo(DH)_2H_2O$ (**10**)	−1.28	Irrev		−1.55		15	−1.441	0.191	−1.577	0.072

[a] From $\log[i/i_l - i]$ versus E.
[b] From CPR.
[c] From cyclic voltammetry data at 0.1 V s^{-1} on Hg stationary electrode: $E_{pc}(\mathbf{I})$ refers to Co(III)/Co(II), $E_{pc}(\mathbf{II})$ refers to Co(II)/Co(I); $\Delta E_p(\mathbf{I}) = E_{pc}(\mathbf{I}) - E_{pa}(\mathbf{I})$, $\Delta E_p(\mathbf{II}) = E_{pc}(\mathbf{II}) - E_{pa}(\mathbf{II})$.

waves is linearly related to the concentration of the complexes up to 2 mM.

From the analysis of the plot of $\log[i/(i_l - i)]$ versus E, wave **I** is associated with an electrochemically quasi-reversible or irreversible process [17], while wave **II** is associated with a reversible process for **6** and **9** and quasi-reversible one for the others. Both processes are monoelectronic, as it was proved by the CPR experiments made on the plateau of the first wave (see below), but for **7**, **8** and **9** the ratio $i_l(\mathbf{I})/i_l(\mathbf{II})$ is about 1 (Fig. 3 (A)), whereas for **5**, **6** and **10** it is greater than 1 (Fig. 3(B)).

The $E_{1/2}$ values relative to the Co(III)/Co(II) electron transfer become 530 mV more negative on going from **5** to **10**; the $E_{1/2}$ values relative to the Co(II)/Co(I) electron transfer follow a more complicated pattern (Fig. 4).

3.4.2. Controlled potential reduction

After exhaustive CPR corresponding to 1 faraday mol^{-1} at the potential of the plateau of the first wave, made under inert gas atmosphere, both the cathodic waves disappear while anodic signals develop: the height of those waves is linearly proportional to the number of Coulombs passed.

The solution from a typical yellow–orange color becomes green–blue and is stable for several minutes under nitrogen atmosphere at ambient temperature. The polarograpy made after the CPR shows the development of new cathodic and anodic waves due to the reduction and oxidation of the products resulting after reduction.

3.4.3. Cyclic voltammetry

The CV results on an Hg drop electrode are in agreement with the polarographic data and are summarized in Table 5. All the examined compounds show a couple of cathodic peaks and each of them is coupled with an anodic partner, at least at sufficiently high scan rate. The first cathodic/anodic peak couple is associated with a mono-electron Co(III)/Co(II) transfer while the second cathodic/anodic peak couple proves another mono-electron transfer that is associated with the Co(II)/Co(I) process at more negative potential (Fig. 3).

For **7**, **8** and **9** CV made at low scan rate (0.1 V s^{-1}) shows that the ratios between the cathodic and anodic current peaks, $I_{pc}(\mathbf{I})/I_{pa}(\mathbf{I})$ and $I_{pc}(\mathbf{I})/I_{pc}(\mathbf{II})$, are about 1 (Fig. 3 (C)), while in the case of **5**, **6** and **10** the ratios $I_{pc}(\mathbf{I})/I_{pa}(\mathbf{I})$ and $I_{pc}(\mathbf{I})/I_{pc}(\mathbf{II})$ are greater than 1 at low scan rates (Fig. 3(D)) and approach 1 as the scan rate increases; meanwhile the $E_{pc}(\mathbf{I})$ shifts towards more positive values [18].

4. Discussion

Present results confirm previous findings [4,5] that in $Co(DBPh_2)_2$ complexes, the nature of the axial ligands

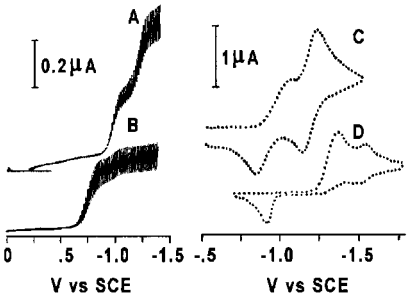

Fig. 3. Polarography in DMSO + 0.1 M TEAP at 25°C of **8** (A) and **5** (B). Cyclic voltammetry in the same solvent of **8** (C) and **10** (D) at a scan rate of 0.1 V s^{-1} on Hg electrode. The concentration of the complexes is about 1 mM.

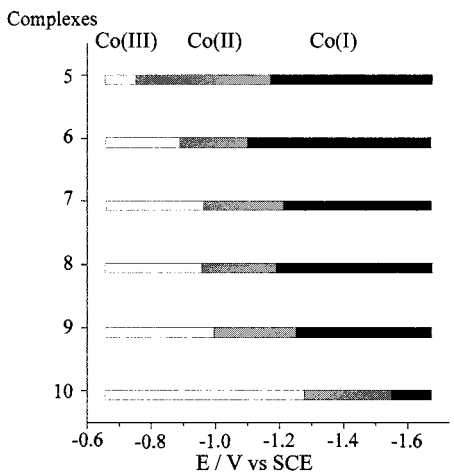

Fig. 4. Schematic representation of the relative stability of the oxidation states Co(III)/Co(II)/Co(I) for the complexes **5**–**10** in DMSO + 0.1 M TEAP at 25°C.

determines the conformation of the equatorial moiety, through their electronic and steric interactions with the BPh_2 groups. When both axial ligands have similar and moderate bulk and display similar electronic interactions with phenyl group, the 'up–down' conformation is the preferred one in the solid state. This implies that planar axial ligands such as *N*-MeIm or Py assume orientation B. This observation suggests that the 'down–down' conformation, which leads to the 'sandwiching' of one axial ligand by the phenyl groups, should be less stable than the 'up–down' conformation unless the latter ligand is involved in strong π–π attractive interactions with the phenyl rings. In this case, the 'down–down' conformation is stabilised by the 'sandwiching' electronic interactions, as found in the $MeCo(DBPh_2)_2TCNE$ (TCNE = tetracyanoethylene) [9]. On the contrary, when the difference in bulk between the two axial ligand increases, the 'up–down' conformation becomes less stable. This is well illustrated by the structures of a series of the $RCo(DBPh_2)_2(NCCH_3)$ complexes, with R having different bulk [9]. For R = Me the 'up–down' conformation is found in the solid state, while the 'down–down' conformation, with both the axial phenyl groups facing the acetonitrile ligand, is observed when $R = n$-Pr and β-styryl. A similar 'down–down' conformation, due to a large difference in bulk between the axial ligands, has also been reported for the octahedral PyFe(II)-$(DBPh_2)_2PPh_2Me$ complex [5f]. The only case in which an 'up–up' conformation is observed is the pentacoordinate Co(I) species, $PyCo(DBF_2)_2^-$ [6], where, because of the lack of the *trans* axial ligand, Py can assume the preferred orientation A, forcing the equatorial moiety into that conformation. Similarly, in $MeCo(DBPh_2)$-(DH)*N*-MeIm and in $MeCo(DBPh_2)$(DH)Py the planar ligand assumes the preferred orientation A, forcing the axial phenyl of the BPh_2 bridge to face the alkyl group. It is of interest to compare the coordination geometry of the MeCo(chel)Py, when chel is varied. The mean values of the Co–N equatorial distances are very similar in the boryl derivatives and shorter than in cobaloximes (Table 6), possibly due to the strong decrease of electron density on the metal center on substitution of the oxime bridges with boryl bridges (see below). Data of Table 6 suggest that the Co–Py distance is longer in orientation B, but for the same orientation it appears to increase slightly in the order $(DB(p\text{-}OCH_3Ph)_2)_2 < (DB(p\text{-}ClPh)_2)_2 < (DBF_2)_2$. This might be indicative of some electronic *cis* influence. The Co–CH_3 distances are very similar in all but one of the complexes of Table 6. The value of 2.032(6) Å in the $(DBp\text{-}OCH_3Ph_2)_2$ derivative is slightly greater than those in the other ones. If significant, such a difference could be attributed to the effect of the *para* methoxy substituent; unfortunately, the corresponding distances in the parent $MeCo(DBPh_2)_2Py$ are not available for a better comparison (see above).

The ^{1}H-NMR spectra suggest that also the distribution of conformations in solution for the $RCo(DH)_2$–$n(DB(p\text{-}XPh)_2)_nN$-MeIm compounds and that observed in the corresponding BPh_2 derivatives are the same, being mainly 'up' and 'up–down' for R = alkyl and 'down' and 'down–down' for R = Ph, respectively. On one hand, the independence of the conformational equilibrium from the phenyl substituents candidates these molecules as suitable systems for studying variations of through-space effects induced by substitution of aromatics and related changes in magnetic anisotropy and bond electric dipoles [19]. On the other hand, it induces a reconsideration of the relative effectiveness of the steric and π–π interactions in determining the conformation of these complexes. Indeed, according to the model of Hunter and Sanders the major contributions to the π–π interactions come from the electrostatic and van der Waals interactions [20]. At interplanar separations greater than 3.4 Å the latter is always attractive and is roughly proportional to the

Table 6
Comparison of coordination geometry for MeCo(chel)Py complexes with several equatorial chel ligands

Complexes	Co–N_{eq} (mean, Å)	Co–Me (Å)	Co–Py (Å)	Orientation
$MeCo(DBF_2)_2Py$ [a]	1.861(13)	2.007(8)	2.119(4)	B
$MeCo(DB(p\text{-}OCH_3Ph)_2)_2Py$	1.867(5)	2.032(6)	2.086(6)	B
$MeCo(DB(p\text{-}ClPh)_2)_2Py$	1.864(8)	1.998(9)	2.106(8)	B
$MeCo(DH)(DBPh_2)Py$	1.873(10)	2.000(11)	2.083(9)	A
$MeCo(DH)_2Py$ [b]	1.899(8)	1.998(6)	2.068(3)	A

[a] From ref. [2].
[b] From ref. [22].

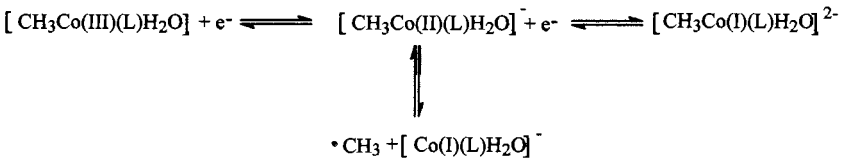

Scheme 3.

area of π–π overlap. The former is very geometry dependent: it varies from attractive for an edge-on or an offset π stacked geometry to repulsive for a face-to-face stacked geometry. The presence of a strongly polarizing group should affect the electron density on the aromatic ring and enhance or relieve the electrostatic repulsion, so influencing the overall geometry of the system. This really happens, for example, in the so-called molecular clips [21]. In the present case the insertion of substituents in the phenyl ring does not cause relevant structural modification, suggesting that more striking variation in the π properties (e.g. the substitution of TCNE for Py as axial ligand) are required in order to alter conformation both in solution and in solid state.

On the contrary, the insertion of a substituent in the phenyl ring affects remarkably both the electronic density at the metal center and the rate of the coupled chemical reaction following the electron transfer. It was already demonstrated that the substitution of O···H···O bridges with BF_2 groups both in cobaloximes and in iminocobaloximes strongly decreases the electron density on the central metal ion [3]. A direct comparison of these data with the present ones is not possible because different solvents have been used. However, data in Table 5 show that, for methylcobaloxime derivatives, the electrochemical behavior of the complexes **6**, **7**, **8**, and **9,** containing $B(p\text{-}XPh)_2$ groups, is intermediate between that of the unsubstituted cobaloxime **10** and that of the complex **5** containing BF_2. Within the series **6**–**9**, the substituents on the aromatic ring also influence the electron density on central Co atom, although to a lesser extent. This effect is of about 100 mV for the first reduction step and about 160 mV for the second one, therefore comparable to that due to a variation of the R group from Me to Ph [3]. On the whole, as the electron-withdrawing power of the equatorial ligand increases, the reduction potentials associated with both Co(III)/Co(II) and Co(II)/Co(I) processes shift towards more positive values, indicating the decrease of electron density on Co atom (Fig. 4). Noticeably, the cobaloxime **10** is stable in the Co(III) oxidation states at potentials at which all the other examined compounds are in the Co(I) oxidation state. The stability range of the Co(II) state is about the same for the complexes **6** and **8** but it slightly increases for the complexes **7**, **9**, **10** and is almost double for the complex **5** (Fig. 4).

The increase of the ratio of the CV peak currents I_{pc}(**II**)/I_{pc}(**I**) up to 1 on increasing the scan rate and the shift of the potentials with the scan rate towards more positive values prove that there is a coupled chemical reaction following the first electron transfer. Furthermore, the disappearance of the second cathodic peak in CV when the CPR is made at the potential of the first one is in agreement with the reaction in Scheme 3 [18]. According to this Scheme the first electron transfer is followed by two competitive reactions, a second monoelectron Co(II)/Co(I) transfer and the homolytic dissociation of the Co–C bond, as it was previously described for a series of organocobaloximes in dimethylformamide [3]. Even if a numerical value for this reaction has not been calculated, the increase of the I_{pc}(**II**)/I_{pc}(**I**) ratio, at constant CV scan rate [18], indicates that the reaction becomes faster in the order $\mathbf{9} \approx \mathbf{8} \approx \mathbf{7} < \mathbf{6} < \mathbf{5} < \mathbf{10}$; therefore, the insertion of $B(p\text{-}XPh)_2$ bridges slows the decomposition reaction in comparison with both the cobaloxime **10** and the complex **5** containing BF_2.

Acknowledgements

We are grateful to CNR (Rome) and to Murst (Rome) for the financial support.

References

[1] (a) G.N. Schrauzer, Chem. Ber. 95 (1962) 1438; (b) F. Umland, D. Thierig, Angew. Chem. Int. Ed. Engl. 1 (1962) 333; (c) G. Schmid, P. Powell, H. Nöth, Chem. Ber. 101 (1968) 1205.
[2] M.S. Ram, C.G. Riordan, G.P.A. Yap, L. Liable-Sands, A.L. Rheingold, A. Marchaj, J.R. Norton, J. Am. Chem. Soc. 119 (1997) 1648.
[3] (a) C. Tavagnacco, G. Balducci, G. Costa, K. Täschler, W. von Philipsborn, Helv. Chim. Acta 73 (1990) 1469; (b) G. Costa, A. Puxeddu, C. Tavagnacco, G. Balducci, R. Kumar, Gazz. Chim. It. 116 (1986) 735; (c) G. Costa, A. Puxeddu, C. Tavagnacco, J. Organomet. Chem. 296 (1985) 161 and refs. therein.
[4] (a) F. Asaro, R. Dreos, S. Geremia, G. Nardin, G. Pellizer, L. Randaccio, G. Tauzher, S. Vuano, J. Organomet. Chem. 548 (1997) 211; (b) R. Dreos, G. Tauzher, S. Vuano, F. Asaro, G. Pellizer, G. Nardin, L. Randaccio, S. Geremia, J. Organometal. Chem. 505 (1995) 135.
[5] (a) M. Verhage, D.A. Hoogwater, H. van Bekkum, J. Reedijk, Recl. Trav. Chim. Pays Bas 101 (1982) 351; (b) D.V. Stynes, D.B.Leznoff, D.G.A.H de Silva, Inorg. Chem. 32 (1993) 3989; (c) G. Impey, D.V. Stynes, J. Am. Chem. Soc. 115 (1993) 7868; (d) D.V. Stynes, Inorg. Chem. 33 (1994) 5022; (e) D.G.A.H. de Silva, D.B. Leznoff, G. Impey, I. Vernik, Z. Jin, D.V. Stynes, Inorg. Chem. 34 (1995) 4015; (f) I. Vernik, D.V. Stynes, Inorg. Chem. 35 (1996) 6210.
[6] S. Shi, L.M. Daniels, J.H. Espenson, Inorg. Chem. 30 (1991) 3407.
[7] (a) N. Bresciani-Pahor, L. Randaccio, E. Zangrando, Inorg. Chim. Acta 168 (1990) 115; (b) S.M. Polson, R. Cini, C. Pifferi, L.G. Marzilli, Inorg. Chem. 36 (1997) 314; (c) L. Randaccio, N. Bresciani-Pahor, E. Zangrando, L.G. Marzilli, Chem. Soc. Rev. 18 (1989) 225.
[8] S. Hirota, S.M. Polson, J.M. Puckett Jr., S.J. Moore, M.B. Mitchell, L.G. Marzilli, Inorg. Chem. 35 (1996) 5646.
[9] R. Dreos, S. Geremia, G. Nardin, L. Randaccio, G. Tauzher, S. Vuano, Inorg. Chim. Acta 272 (1998) 74.
[10] G.N. Schrauzer, in: R. Parry (Ed.), Inorganic Syntheses, vol. 11, 1968, p.61 ff.
[11] T.P. Povlock, W.T. Lippincott, J. Am. Chem. Soc. 80 (1958) 5409.
[12] (a) G.M. Sheldrick, SHELXS-86, Program for Structure Solution, Acta Crystallogr. Sect. A 46 (1990) 467; G.M. Sheldrick, Program for Structure Refinement, Universität Göttingen, Göttingen, Germany, 1993.
[13] J.A. Riddick, in: A. Weissberger, E.S. Proskaue (Eds.), Organic Solvents. Physical Properties and Methods of Purification, Wiley–Interscience, New York, 1970, p. XIII.
[14] D. Britz, Electrochim. Acta 25 (1980) 1449.
[15] R. Dreos, G. Nardin, L. Randaccio, G. Tauzher, S. Vuano, Croat. Chim. Acta 72 (1999) 231.
[16] L.M. Jackman, S. Sternhell, Application of Nuclear Magnetic Resonance Spectroscopy in Organic Chemistry, Pergamon Press, Oxford, second Ed., 1969, p. 202.
[17] J. Heyrovsky, J. Kuta, Principles of Polarography, Academic Press, New York, 1966.
[18] A.J. Bard, L.R. Faulkner, Electrochemical Methods, Wiley, New York, 1980.
[19] J. Jusélius, D. Sundholm, Phys. Chem. Chem. Phys. 1 (1999) 3429.
[20] C.A. Hunter, J.K.M. Sanders, J. Am. Chem. Soc. 112 (1990) 5525.
[21] J.N.H. Reek, A.H. Priem, H. Engelkamp, A.E. Rowan, J.A.A.W. Elemans, R.J.M. Nolte, J. Am. Chem. Soc. 119 (1997) 9956.
[22] A. Bigotto, E. Zangrando, L. Randaccio, J. Chem. Soc. Dalton Trans. (1976) 96.